Quaternary Research 83 (2015) 307–314

Contents lists available at ScienceDirect

Quaternary Research

journal homepage: www.elsevier.com/locate/yqres

Late Holocene Indian summer monsoon variations recorded at Lake Erhai, Southwestern China

Hai Xu [a,*], Xinying Zhou [b], Jianghu Lan [a], Bin Liu [a], Enguo Sheng [a], Keke Yu [a], Peng Cheng [a], Feng Wu [a], Bin Hong [c], Kevin M. Yeager [d], Sheng Xu [e]

[a] State key Laboratory of Loess and Quaternary Geology, Institute of Earth Environment, Chinese Academy of Sciences, Xi'an, China
[b] Laboratory of Human Evolution and Archeological Science, Institute of Vertebrate Paleontology and Paleoanthropology, Chinese Academy of Sciences, Beijing, China
[c] State Key Laboratory of Environmental Geochemistry, Institute of Geochemistry, Chinese Academy of Sciences, Guiyang, China
[d] Department of Earth and Environmental Sciences, University of KY, Lexington KY40506, USA
[e] Scottish Universities Environmental Research Centre, East Kilbride, Glasgow G75 0QF, United Kingdom

ARTICLE INFO

Article history:
Received 22 May 2014
Available online 14 January 2015

Keywords:
Lake Erhai in southwestern China
Indian summer monsoon
Precipitation
Late Holocene
Medieval period

ABSTRACT

In this study we report changes in Indian summer monsoon (ISM) intensity during the past ~3500 yr inferred from proxy indices at Lake Erhai, southwestern China. Both the pollen concentrations and other proxy indices, including sediment grain size, total organic carbon contents (TOC), and elemental contents (e.g., Fe, Al), clearly indicate a long term decreasing trend in ISM intensity over the late Holocene. During the period from approximately AD 750 to AD 1200, pollen concentrations of conifer and broadleaf trees, and herbs reached the lowest levels over the past ~3500 yr; while the pollen percentages of both herbs and broadleaf trees increased, suggesting a significant medieval drought. The grain size, TOC, and elemental contents also support an arid climate during the medieval period. The Little Ice Age (LIA) at Lake Erhai was characterized as cold and wet. The medieval and LIA climatic patterns at Lake Erhai were similar to those over most of the ISM areas, but anti-phase with those over East Asian summer monsoon (EASM) areas. We suspect that sea surface temperature variations in the Indo-Pacific oceans and the related land-sea thermal contrasts may be responsible for such hydroclimatic differences between EASM and ISM areas.

Introduction

The Indian summer monsoon (ISM) plays an important role in influencing population, economies, and cultural development. Knowledge of the changes in ISM intensity during the late Holocene is critical in understanding the underlying mechanisms and in predicting regional/local changes in monsoon precipitation. Lines of evidence have revealed several remarkable episodes in the past ~2000 yr, e.g., the medieval period, the Little Ice Age (LIA), and the most recent 100–200 yr, during which the ISM has experienced large and significant changes. Among those climatic episodes, the medieval period received the most attention because climatic changes during this period are important to understanding the natural and anthropogenic driving forcings of the recent warming. This is because the medieval period, which has been suggested to have been generally warm by multiple lines of evidence (e.g., Stine, 1994; Graham et al., 2011; Diaz et al., 2011; Laird et al., 2012), is analogous to modern warming, but anthropogenic impacts were minor and weak relative to today. Although lines of evidence suggest that broadly warmer conditions may have prevailed during the medieval period, changes in precipitation appear to have varied regionally (Graham et al., 2011; Diaz et al., 2011). For example, droughts occurred over much of the ISM areas, like equatorial East Africa (Verschuren et al., 2000; Thompson et al., 2002), southern China (Chu et al., 2002), and south China Sea (Sun et al., 2012). Meanwhile, over the East Asian summer monsoon (EASM) areas, like northern China, a considerable body of evidence indicates that a warm and wet climate occurred during the medieval period (e.g., Zhou et al., 2011, and references therein). Wetter climatic conditions have also been reported during this time in central (Adhikari and Kumon, 2001) and northern Japan (Yamada et al., 2010). Such hydroclimatic contrasts may also have existed during the LIA and the recent 100–200 yr. Clearly, it is necessary to develop more evidence for a clearer view of the hydroclimatic contrasts over ISM and EASM areas, and to understand the controlling mechanisms.

Lake Erhai is located in the northwest Yunnan province, China, on the southeastern Tibet plateau (Fig. 1). The climatic changes around this region are sensitive to variations in ISM intensity (e.g., Shen et al., 2005; An et al., 2011; Chen et al., 2014). Although relatively long-term climatic and ecological changes at Lake Erhai have been studied (Shen et al., 2005, 2006; Dearing et al., 2008), short-term variations have

* Corresponding author at: Fenghui South Road, #10, Xi'an, Shaanxi province, 710075, China. Fax: +86 29 6233 6295.
E-mail address: xuhai2003@263.net (H. Xu).

http://dx.doi.org/10.1016/j.yqres.2014.12.004
0033-5894/

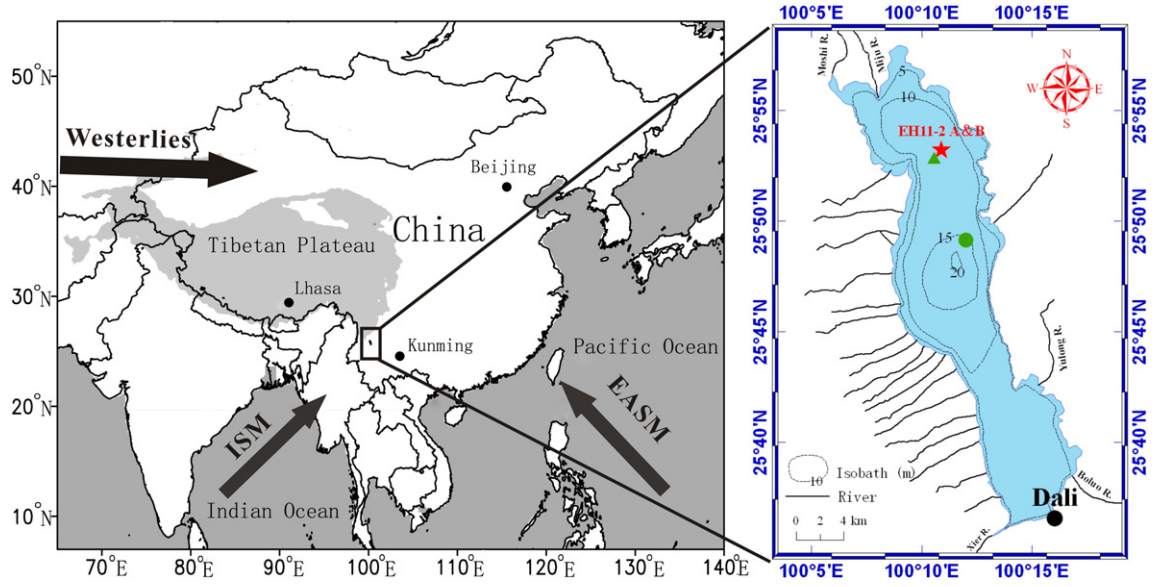

Figure 1. Sampling site at Lake Erhai, southwestern China. Red star shows locations of cores EH11-2 A, and 2B in this study. The green circle and triangle show locations of cores by Hyodo et al. (1999) and Shen et al. (2006), respectively. Rivers in Lake Erhai catchment (right panel) were redrawn from Shen et al. (2006). The grey shading over southwestern China represents the Tibetan Plateau.

been less well constrained. For example, more work is needed to address changing climatic patterns during the medieval period, and understand how regional ecology responded. Here we studied high-resolution proxy records of climatic changes at Lake Erhai over the late Holocene and discussed the possible causes.

Background and methods

Background

Lake Erhai is a pull-apart rift lake. The mean annual temperature is 15.1 °C and the mean annual precipitation is 1060 mm (at Dali meteorological station). More than 85% of the annual precipitation is delivered from May to October. Lake water is supplied mainly by precipitation and snow melt. A large number of small rivers are distributed around the lake (Fig. 1; see Shen et al., 2006 for details). Bedrock in the catchment mainly consists of schist, gneiss, and calcareous conglomerates (Xu et al., 1999). Fir (*Abies delavayi*) and pine trees (mainly *Pinus yunnanensis* and *Pinus armandi*) are widely distributed between 2500 and 3500 m elevations within the catchment (Ming and Fang, 1982). Shrubs such as Rhododendron are distributed predominantly in the eastern catchment. Eucalyptuses are also common.

Sampling

Surface sediment cores were collected with a gravity corer from the northern part of the lake (with 100% sediment recovery) in 2011. Core EH11-2A, and 2B (25°53.226′ N; 100°10.890′ E; water depth: 12 m) are 125 and 127 cm long, respectively. Sediment lithologies of both cores correlate well; the upper ~60 cm of the cores was gray-blackish in color, while the lower sections were cyan-grayish in color. Samples from core EH11-2B were prepared at every 0.5 cm for the upper 39 cm and at every 1 cm for the remainder of the section; while those from core EH11-2A were prepared at 1-cm intervals.

Methods

Dating

The radioactivities of ^{137}Cs and ^{210}Pb (Fig. 2) were determined for the upper 25 cm of core EH11-2B using an Ortec Germanium (HPGe) well detector (GWL-15-250). Snail shells (*Erhaiini*) were found at intervals of 83–64 cm and 127–112 cm in core EH11-2B, and were selected for ^{14}C dating (Fig. 3). We also chose samples at 55 cm and 127 cm in core EH11-2B for ^{14}C dating, based on bulk organic matter after removal of the carbonates (by treatment with dilute HCl). To quantify the presence of an "old" carbon effect, we also determined ^{14}C ages of the lake

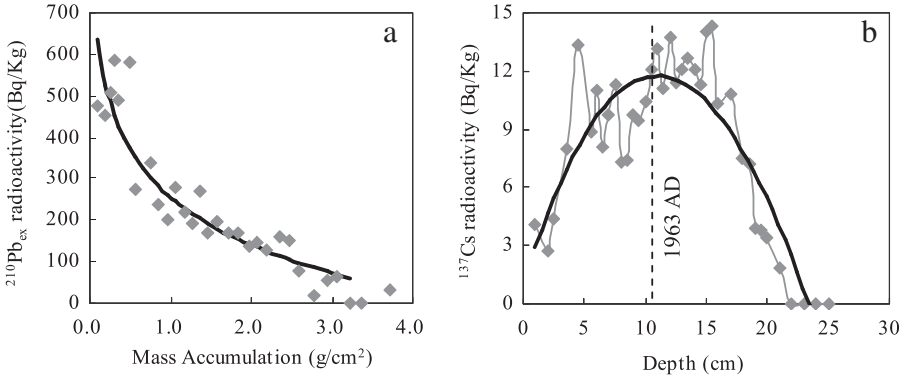

Figure 2. ^{210}Pb (a) and ^{137}Cs (b) activity concentrations from core EH11-2B. Lines in panel a and b denote the logarithmic and polynomial regression, respectively.

https://doi.org/10.1016/j.yqres.2014.12.004 Published online by Cambridge University Press

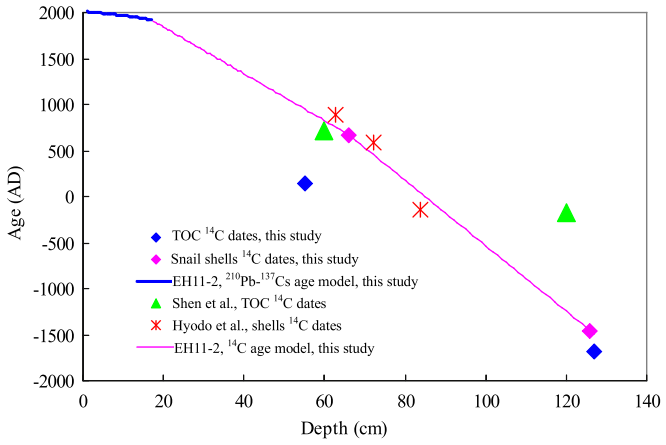

Figure 3. Age model of core EH11-2B. Ages of the upper 17 cm sediments (0–17 cm) were derived from ^{210}Pb and ^{137}Cs ages. Ages below 17 cm were derived from a combination of the ^{210}Pb–^{137}Cs ages and the corrected ^{14}C ages of the snail shells. Red crosses show the calibrated ^{14}C ages of snail shells from Hyodo et al. (1999) after correcting for the old carbon effect (Table 1); green triangles show the calibrated TOC-^{14}C ages after correcting for the old carbon effect (Table 1; see the text for details).

water, living snails, and living submerged pondweeds (predominantly *Potamogetonaceae*; see ^{14}C age model).

Measurement of proxy indices

Elemental contents of core EH11-2A (Fig. 4) were measured using an X-ray fluorescence spectrometer (XRF, Axios advanced, PW 4400). Pollen concentrations of core EH11-2B were analyzed using the method described by Li et al. (2006). Magnetic susceptibility (MS) of core EH11-2B was determined by a Bartington Meter (Model MS2). Bulk carbonate contents (carb%) of core EH11-2B were determined by titration with dilute HCl. The remaining sediments were rinsed to neutral pH, and then the total organic carbon (TOC) and total nitrogen contents were measured with an elemental analyzer (vario MACRO cube, Elementar, Germany), with an experimental error of <0.5%. C/N ratios were then calculated. Sediment samples of core EH11-2B were pretreated with H_2O_2 to remove organic matter, and then grain size was measured with a laser particle size analyzer (Malvern 2000, England), with an experimental error of <3%. Biogenic silica contents (BSi%; core EH11-2B) were determined using an alkaline-extraction method (Liu et al., 2014a).

Results

^{210}Pb and ^{137}Cs dating

Both the low ^{137}Cs radioactivities and the pattern of the ^{137}Cs profile of core EH11-2B (Fig. 2) are similar to those from previous work at Lake Erhai (e.g., Zhang et al., 1993; Xu et al., 1999). The ^{137}Cs radioactivities in core EH11-2B increased sharply at ~17 cm, which is also similar to the results of Wang et al. (2012). The shape of the ^{137}Cs profile may be influenced by some local limnological processes, including mixing of the surface sediments; but the central peak will not be moved (e.g., Xu et al., 2010b). We assign the date of 1963 to the center of the ^{137}Cs best fit (at 10.5 cm) (Fig. 2b).

The fit of the excess ^{210}Pb radioactivities at Lake Erhai exhibits a classical logarithmic pattern (Fig. 2a), which is also similar to the results of previous work there (e.g., Xu et al., 1999). The ^{210}Pb dating results are generally consistent with the ^{137}Cs dating results. For example, at 10.5 cm, the ^{210}Pb ages produced using the constant initial concentration (CIC) and constant rate of supply (CRS) models (Goldberg, 1963; Robbins and Edgington, 1975; Appleby, 1978) are AD 1964.6 and AD 1969, respectively, both of which are similar to the assigned ^{137}Cs date (AD 1963). We obtained the age model of the upper 17 cm by averaging the ^{137}Cs and ^{210}Pb-CIC ages. Eucalyptus trees were introduced to southwestern China from Australia around the beginning of the 20th century (Zhang et al., 2007). Therefore, eucalyptus pollen can be used as another time-marker at Lake Erhai. In this study, eucalyptus pollen was identified in the upper 15 cm of sediment in core EH11-2B (Figs. 5, 6); while no eucalyptus pollen was found below 15 cm. The age determined at 15 cm is approximately AD 1934, which is consistent with the occurrence of the eucalyptus pollen and strongly supports the ^{137}Cs-^{210}Pb dating model.

^{14}C age model

As shown in Table 1, the calibrated ^{14}C age of the lake water is 702 cal yr BP (Table 1; median probability). The calibrated ^{14}C ages of the living snails and living submerged plants are 523 and 610 cal yr BP, respectively, both of which are close to the calibrated ^{14}C age of the lake water. These data clearly indicate an old carbon effect in Lake Erhai. Depending on local hydrological and climatic conditions, the old carbon effect may vary with time. Due to the lack of such information at Lake Erhai, relatively constant old carbon effects are assumed during the past 3500 yr. Thus, the corrected ^{14}C ages of the snail remains are the ^{14}C ages minus that of the living snails (523 cal yr BP); while the ^{14}C ages of the bulk organic matter are corrected against the ^{14}C age of the living submerged plants (610 cal yr BP). Xu and Zheng (2003) carried out a comprehensive study of the ^{14}C ages of different organic factions in the sediments of Lake Erhai, and found considerable differences in the ^{14}C ages of different organic fractions. Considering the complexity of organic matter ^{14}C ages at Lake Erhai, we established our age model based on the ^{210}Pb–^{137}Cs ages, and the corrected ^{14}C ages of the snail remains (see below).

We used the average ^{210}Pb–^{137}Cs age at 17 cm (AD 1916.6) as the first age-controlling point. We then used the corrected snail shell ^{14}C ages at 66 and 126 cm (Table 1) as additional dated points: AD 673 and 1458 BC, respectively. Then the dating model of core EH11-2B below 17 cm was obtained by linear interpolation between these three points (Fig. 3). Core EH11-2A shares the same age model with core EH11-2B as both were collected from the same site. Hyodo et al. (1999) also established a dating model for Lake Erhai sediment (core ER3) based on calibrated ^{14}C ages of snail shells. However, their ^{14}C ages were not corrected for the old carbon effect. As shown in Figure 3, after removal of the old carbon effect (523 yr), the corrected snail-shell ^{14}C ages of Hyodo et al. (1999) correlate well with the age model of this study. The TOC ^{14}C ages of this study and those of Shen et al. (2006; after an old carbon correction of 610 yr) are also plotted. As shown in Figure 3, some of these TOC ^{14}C ages agree with our dating model, and others do not, consistent with Xu and Zheng's (2003) viewpoint that "*special caution is necessary when radiocarbon ages of bulk sediments are used*" in Lake Erhai sediments.

Results of the proxy measurements

Grain size, carb%, elements, MS

Sediment grain size (mean value, and hereafter) shows a general decreasing trend from ~900 BC to AD 750. It was fine (~10 μm) and relatively constant from AD 750 to AD 1400, and increased after AD 1400 (Fig. 4). The carb% shows a similar trend as the grain size (Fig. 4). Rb/Sr ratios are generally inversely correlated with grain size and carb%. Concentrations of some primary crustal elements, including Fe and Al, also show long term trends similar to the Rb/Sr ratios (Fig. 4). The magnetic susceptibility increased sharply after ~AD 750, and kept increasing to ~AD 1750; after ~AD 1750, MS showed a decreasing trend (Fig. 4).

TOC and C/N ratios

TOC percentages were relatively steady from 1500 BC to AD 500, and then decreased, and stabilized at relatively low values from about

https://doi.org/10.1016/j.yqres.2014.12.004 Published online by Cambridge University Press

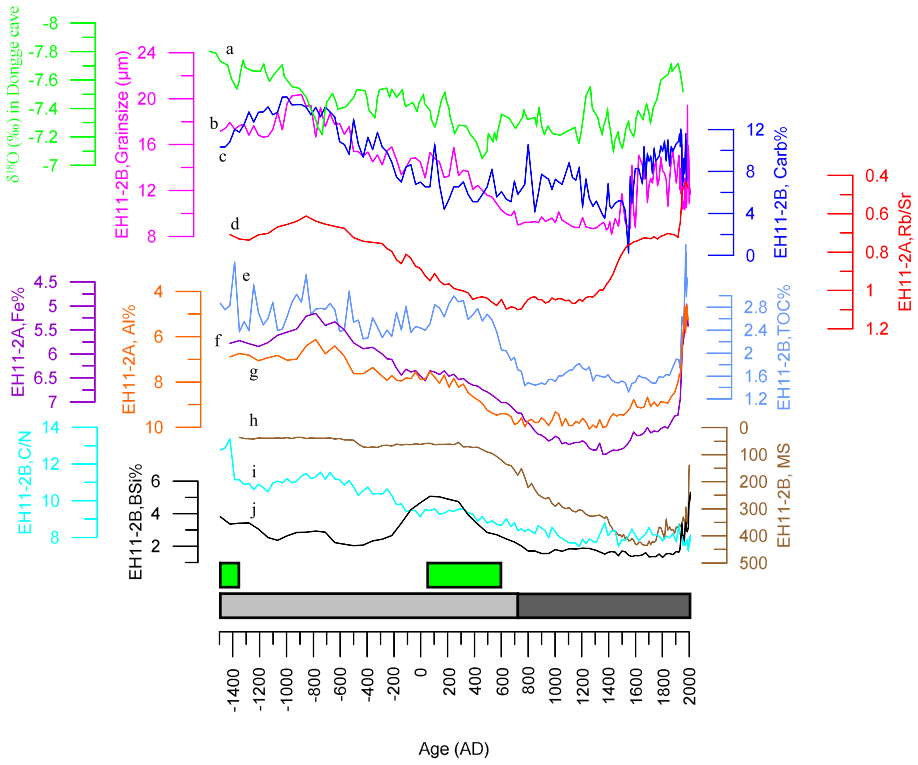

Figure 4. Comparison of proxy indices in Erhai sediment cores and stalagmite $\delta^{18}O$ of Dongge cave (curve a; green; Wang et al., 2005). Curve b (pink): grainsize; c (blue): carbonate content; d (red): Rb/Sr ratios; e. (light blue) TOC; f (purple): Fe%; g (orange): Al%; h (brown): magnetic susceptibility; i (cyan) C/N ratios; j (black): biogenic silicon contents. The grey-blackish and cyan-grayish rectangles indicate different colors of the core; while the green shaded rectangles indicate the occurrences of snail remains in the core.

AD 750 to AD 1900. After AD 1900, TOC percentages increased rapidly (Fig. 4). The total nitrogen of lake sediments shows a trend similar to TOC (figure not shown). C/N ratios exhibit a clear decreasing trend during the past 3500 yr, which is similar to the results of Zhang et al. (2000). The BSi% curve generally shows a trend similar to TOC.

Pollen records

Total pollen concentrations, and pollen concentrations of conifer and broadleaf trees, and herbs exhibit long-term decreasing trends over the late Holocene, except for the past 100–200 yr (Fig. 5). The pollen concentrations of conifer and broadleaf trees, as well as herbs, were higher between 1500 BC and AD 0, after which they began declining, and reached the lowest concentrations between ~AD 750 and AD 1400 (Fig. 5). Between approximately 400 BC and AD 100, the pollen concentrations of both conifer and broadleaf trees reached their maximum (Fig. 5), which is broadly synchronous with high BSi% values in lake sediment (Fig. 4).

Pollen percentages of the conifer trees (e.g., *Pinus*) show similar long-term trends as the corresponding pollen concentration, i.e., broadly decreasing over the late Holocene (Fig. 6). As the proportion of conifer trees decreases, herbs and some drought-tolerant broadleaf trees, such as *Alnus*, would comprise an increasing proportion. As a result, the pollen percentage of the herbs shows an increasing trend during the past 3500 yr; while that of the broadleaf trees been relatively steady (Fig. 6).

Discussion

Climatic significance of the proxy indices

Since Lake Erhai is a hydrologically open lake, the lake level would be relatively steady over the late Holocene (e.g., Chen et al., 2000). Therefore, the grain size of the lake sediments should be mainly controlled by the volume and intensity of runoff, and quantity of river discharge to the lake (e.g., Chen et al., 2000). Increases in runoff and discharge will transport more sediment to the lake, and will increase the coarse fraction of terrestrial sediments, and vice versa. Since runoff and river discharge intensity at Lake Erhai are dominated by the monsoon intensity, the grain size can be used as one indicator of ISM intensity.

Rb generally co-exists with K in K-rich minerals, such as K-feldspar and biotite; while Sr tends to be enriched in Ca-bearing minerals, which are often more easily broken down as compared to K-bearing minerals. Consequently, Rb and Sr are widely used to indicate the intensity of chemical weathering (Xu et al., 2010a; An et al., 2011; Zeng et al., 2013). Stronger chemical weathering in the Lake Erhai catchment results in a greater influx of Sr to the lake, and results in lower Rb/Sr ratios in lake sediments, and vice versa. As a result, the Rb/Sr ratios in Lake Erhai sediment can be used to indicate the intensity of chemical weathering in the lake's catchment, and the ISM intensity (e.g., An et al., 2011). Both Al and Fe, as constituents of primary rock-forming minerals, can be utilized to indicate changes in runoff intensity and river discharge over time, and to indicate changes in monsoon intensity.

Vascular plants are rich in fiber but are low in protein, and therefore organic matter derived from them has high atomic C/N ratios (Meyers, 2003; Xu et al., 2014). In contrast, algae and plankton are relatively protein-rich, and hence exhibit low atomic C/N ratios (Meyers, 2003). The variations in C/N ratio of organic matter in lake sediments are therefore widely used to evaluate the relative contributions of terrestrial organic matter, and lacustrine organic matter in lake sediments.

The climatic significance of the pollen data may be variable on different spatial and temporal scales. Because *Abies* and *Picea* favor shaded, cool and wet environments, and are sensitive to strong droughts (Li and Walker, 1986; Zhou and Li, 2012), and because the fir and pine trees around Lake Erhai are selectively distributed within a cool

https://doi.org/10.1016/j.yqres.2014.12.004 Published online by Cambridge University Press

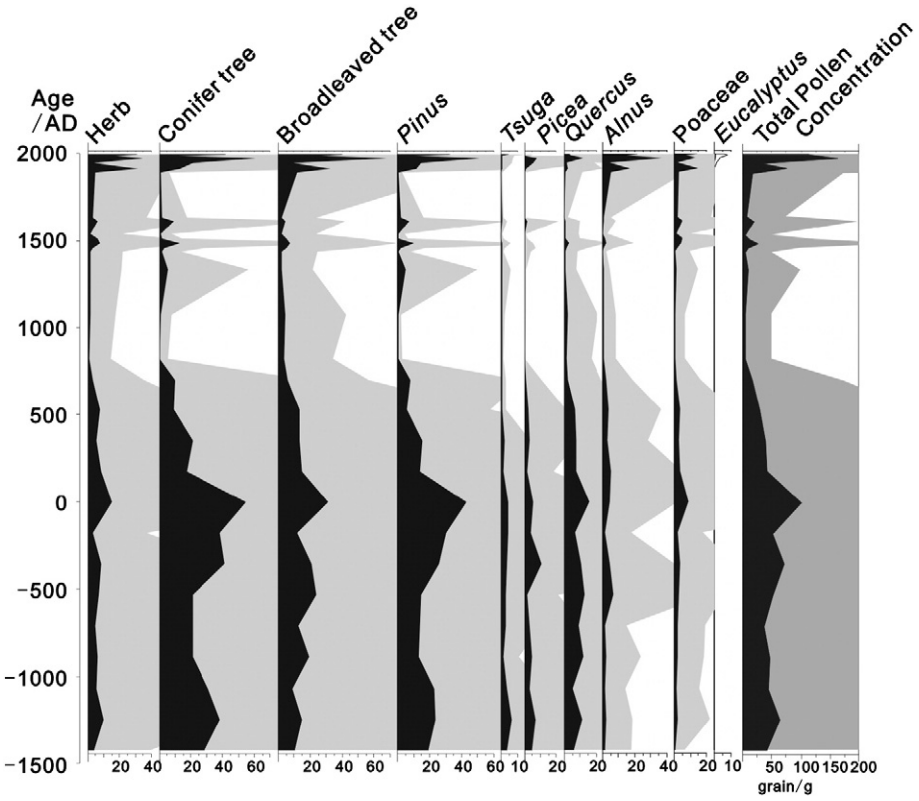

Figure 5. Pollen concentrations of core EH11-2B. The grey shadings denote the exaggeration (×10) of the corresponding data.

elevation zone (2500–3500 m; e.g., Shen et al., 2006), fluctuations in their abundances on short term time scales (like decadal/multi-decadal timescales) are most likely to be primarily controlled by variations in precipitation. Meanwhile, the indigenous herbs prefer relatively arid environments. As a result, when it is drier, the relative abundance of conifer trees would decrease, while that of the herbs would increase, and vice versa. *Quercus* (Oak) and *Alnus* (Alder) generally have high drought tolerance (Li and Walker, 1986; Schrader et al., 2005), and their abundances are mainly controlled by temperature variations on decadal/multi-decadal time scales.

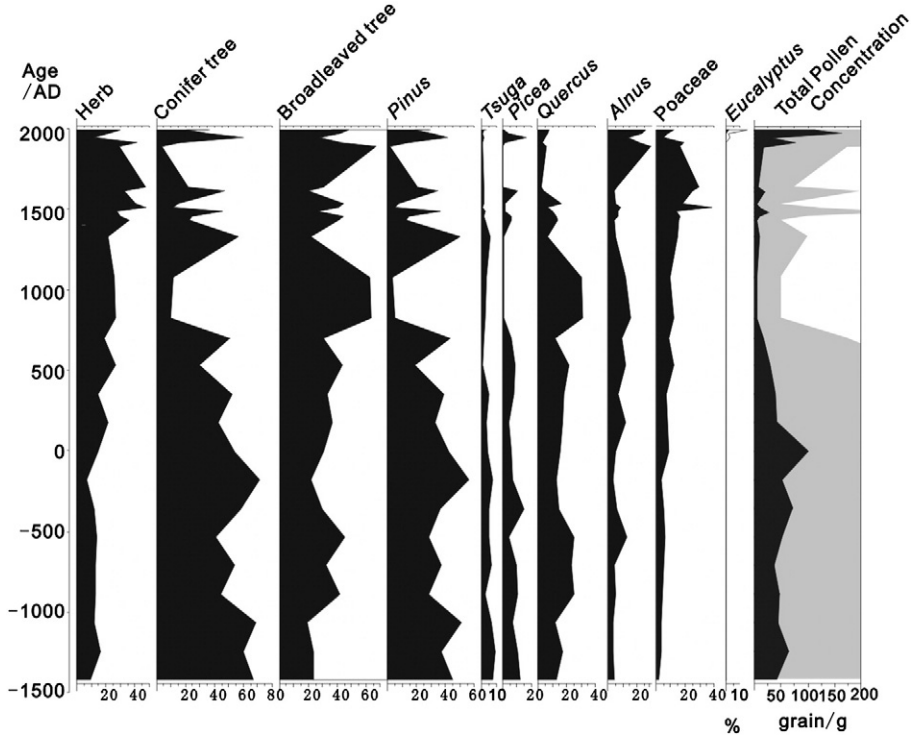

Figure 6. Pollen percentages, and total pollen concentration in core EH11-2B. The grey shadings denote the exaggeration (×10) of the corresponding data.

https://doi.org/10.1016/j.yqres.2014.12.004 Published online by Cambridge University Press

Table 1
^{14}C dating for different samples in Lake Erhai.

Lab code	Sample code	Depth (cm)	Dating materials	Uncalibrated ^{14}C age ± error (^{14}C yr BP)	Calib. age range, 2σ (cal yr BP) (prob.)	Calib. age, 2σ median prob. (cal yr BP) [a]	Corrected ages, (yr BP [b])	Dates (AD/BC)
XA7992	EH120702-4	/	Lake water	770 ± 40	661–745 (0.97)	702	/	
XA7950	EH12-2	/	Submerged pondweeds	656 ± 41	553–613 (0.52) 619–675 (0.48)	610	/	
XA7869	EH120702-1	/	Living snail	492 ± 26	505–541 (1)	523	/	
XA7856	EH11-2-B2-27	66	Snail shell	1863 ± 31	1720–1873 (1)	1800	1277	673
XA7872	EH11-2-B2-87	126	Snail shell	3621 ± 25	3850–3985 (0.99)	3931	3408	-1458
XA6913	EH11-2-B2-16	55	Sediment, TOC	2388 ± 29	2344–2488 (0.96)	2415	1805	145
XA6912	EH11-2-B2-88	127	Sediment, TOC	3836 ± 26	4150–4300 (0.86)	4238	3628	-1678

[a]The calibrated ^{14}C ages were calibrated using the program Calib 6.0.1 (Stuiver et al., 1998), and the median probability (prob.) values were used in this study.
[b]The final ^{14}C ages of the snail remains were corrected against the ^{14}C age of the living snail shells; the final ^{14}C ages of the TOC in lake sediments were corrected against the ^{14}C age of the submerged pondweeds.

Long term climate trends of the late Holocene

Both the trends in pollen concentrations of conifer trees, broadleaf trees, and herbs (Fig. 5), and the corresponding trends in pollen percentages (Fig. 6), reflect a decreasing trend in ISM intensity over the late Holocene. The grain size data also exhibit a general decreasing trend during the past 3500 yr, further suggesting a decreasing ISM intensity. The stalagmite δ^{18}O curve from Dongge cave has been widely used as an indicator of Asian summer monsoon precipitation (Wang et al., 2005). As shown in Figure 4, the stalagmite δ^{18}O data also suggest a long term decreasing trend in ISM intensity, consistent with that inferred from proxy indices at Lake Erhai.

As ISM intensity declined, terrestrial organic matter loading to the lake also declined, resulting in a long term decreasing trend in TOC concentrations in lake sediments (Fig. 4). However, the total biomass within the lake may have remained relatively steady, and if so, the organic matter produced within the lake would comprise a higher fraction of the bulk organic matter in lake sediments. Since the C/N ratio of lacustrine organic matter is much lower than that of terrestrial organic matter (Meyers, 2003; Xu et al., 2006), the C/N ratio of bulk lake sediments would also decrease. This is consistent with the trend of C/N ratio values as shown in Figure 4. In addition, since lake algae and plankton partly utilize dissolved inorganic carbon (DIC) to synthesize organic matter, their organic matter δ^{13}C values would be much higher than those of terrestrial organic matter. We measured δ^{13}C ratios of submerged and emergent plants in Lake Xihu (located about 10 km northwest of Lake Erhai), and found that the average δ^{13}C of submerged plants was about −13.09‰, while that of the emergent reeds was −27.31‰, strongly supporting such an inference. Therefore, the trend in δ^{13}C of the bulk organic matter in lake sediments would also increase corresponding to an increasing contribution of organic matter produced within the lake. This is also consistent with the results of Shen et al. (2005).

Decreased ISM intensity over the late Holocene led to weaker chemical weathering, which is reflected in the increasing trend of Rb/Sr ratio values (during approximately 800 BC to AD 1400; Fig. 4). Concentrations of Fe and Al show broadly increasing trends from 800 BC to AD 1400 (Fig. 4), which can be ascribed to the decreasing fraction of bulk organic matter and bulk carbonate contents in lake sediments, also supporting a decreasing trend in ISM intensity during this period. Chen et al. (2000) reported δ^{13}C and δ^{18}O data from bulk carbonates in Lake Erhai sediments during the period of AD 1290 to AD 1990, and found relatively negative values for both isotopes (−13.6‰ – −5.7‰ for δ^{18}O, and −7.9‰ – −1.6‰ for δ^{13}C), suggesting that the carbonates were mainly chemical/biogenic deposits within the lake. Weaker ISM resulted in lower runoff and lower water salinities due to weaker chemical weathering, which would eventually have led to fewer chemical deposits within the lake. As shown in Figure 4, the carb% in lake sediments exhibits a similar long term trend to that of the grain size, suggesting again a long term decreasing trend in ISM intensity over the late Holocene.

Climates during the Roman and medieval periods, and the Little Ice Age

The Roman period

The biogenic silica content of lake sediment (Fig. 4) was much higher from about 100 BC to AD 400. Meanwhile, both the pollen concentrations (Fig. 5) and percentages (Fig. 6) were also elevated during the period from approximately 400BC to AD 100. These data indicate an increase in biomass both within the lake and the catchment, suggesting that the climate was more favorable during this period. This favorable period coincides with the Roman warm period in Europe (e.g., Bianchi and McCave, 1999; Wang et al., 2013), which has also been suggested to have occurred in Asia (e.g., Yang et al., 2004, 2009; Ji et al., 2005).

The medieval period

As shown in Figure 5, from about AD 750 to AD 1200, the pollen concentrations of both conifer (e.g., *Pinus*) and broadleaf trees (e.g., *Quercus* and *Alnus*) decreased considerably. The total pollen concentration was lower during this interval than at any other time over the past 3500 yr. The conifer trees declined more seriously, as inferred from the relative increases of the pollen percentages of broadleaf trees (Fig. 6). This contrast suggests a severe, dry climatic condition during the medieval period. The grain size remained consistently fine from AD 750 to AD 1400 (Fig. 4), suggesting that runoff and riverine discharge to the lake were significantly lower during that interval. TOC concentrations decreased to their lowest values over the period of record, and remained steady during this interval, suggesting that vegetation cover within the catchment was reduced (Fig. 4). All of these lines of evidence suggest that the ISM intensity was weak during the medieval interval, as has been illustrated in other ISM regions (e.g., Diaz et al., 2011; Graham et al., 2011).

Little Ice Age

During the interval of approximately AD 1450–1850, pollen concentrations of conifer and broadleaf trees remained low (Fig. 5); and the relative pollen percentages of conifer trees, like *pinus,* also declined (Fig. 6). These data suggest cold climatic conditions during this interval, which falls within the traditional LIA period in China. However, both the pollen concentration (Fig. 5) and percentage (Fig. 6) of the herbs, as well as the total pollen concentrations (Fig. 5), increased relatively during this period, suggesting a relatively wet environment as compared with that during the medieval period. Such a relatively wet climatic condition may be ascribed to decreased evaporation under lower temperatures and/or to increased monsoon precipitations. The grain size and carb% increased after ~AD 1450; while the concentrations of Fe and Al, as well as the Rb/Sr ratio, decreased during this period (Fig. 4), suggesting that monsoon precipitation may have increased slightly after ~AD 1450. As shown in Figure 4, monsoon precipitation also increased over the past ~500 yr as inferred from δ^{18}O data from Dongge cave (Fig. 4), consistent with the results from Lake Erhai.

https://doi.org/10.1016/j.yqres.2014.12.004 Published online by Cambridge University Press

Recent climatic changes and human activities

Concentrations of TOC and BSi% increased sharply during the past century. Since multiple lines of evidence indicate a decline in ISM precipitation during the past 100 to 200 yr (e.g., Xu et al., 2012, 2014), these increases cannot be explained by decreased monsoon precipitation, but are most likely a function of increasing human activities during this time. Increasing human activities in the Lake Erhai catchment have resulted in increased nutrient supply to the lake, and consequent increases in primary productivity. Human activities have also resulted in strengthened chemical weathering, for example, as a result of air pollution (lowering pH of precipitation via carbonic and sulfuric acid) associated with industrialization, which has been well-documented throughout China (e.g., Xu and Liu, 2007; Chetelat et al., 2008; Li et al., 2008). This has produced a clear decrease in Rb/Sr ratio values in the lake sediment (Fig. 4). More coarse sediments were brought into the lake due to enhanced human activities (Shen et al., 2005), resulting in an obvious increase in grain size (Fig. 4). Since primary production within the lake increased, the relative proportions of Fe and Al have been diluted (Fig. 4). Increased primary productivity may also result in decreased dissolved oxygen concentrations in lake water, and eventually change the aquatic ecosystems (Zhao et al., 2011). For example, the decreased abundances of aboriginal snails in Lake Erhai today may be ascribed to such a decrease in dissolved oxygen concentration in lake water (Zhao et al., 2011).

Hydrological contrasts between ISM and EASM areas

As mentioned above, the medieval period was dry around Lake Erhai. This relatively dry interval has also been documented in other ISM areas (Graham et al., 2011; Diaz et al., 2011), including Eastern Africa (Verschuren et al., 2000; Thompson et al., 2002), Southern China (Tong et al., 1997; Chu et al., 2002), and the South China Sea (e.g., Sun et al., 2012). We reviewed a number of previous studies and found that there prevailed a broadly "warm-wet" medieval optimum over EASM areas. For example, from northern to northeastern China, and from central to northern Japan, warm and wet climatic conditions can be inferred from peatland/lake sediments (e.g., Ren, 1998; Adhikari and Kumon, 2001; Zhang et al., 2009; Yamada et al., 2010), tree ring records (Zhang et al., 2003; Liu et al., 2009), desert records (Wu and Lu, 2005; Zhou et al., 2008), as well as from historical literature (Zhang, 1994; Ge et al., 2002). These results collectively suggest a broad hydroclimatic contrast during the medieval period between ISM and EASM areas. However, such hydroclimatic contrast may not uniformly cover the whole medieval period; evidence also suggests that there are some specific intervals (within the medieval period) during which both the EASM and ISM areas were possibly dry (e.g., Liu et al., 2014b). Clearly, more evidence is necessary for deep understanding of the medieval hydroclimatic contrasts between EASM and ISM areas.

The relatively wet climatic condition at Lake Erhai during the LIA is also similar to those over other ISM areas, e.g., Eastern Africa (Verschuren et al., 2000), southern China (Chu et al., 2002), and the South China Sea (Sun et al., 2012). However, over typical EASM areas, climate during the LIA has been reported as relatively dry (e.g., Zhang et al., 2003; Tan et al., 2011), which also contrasts with the hydroclimatic pattern over ISM areas. We suspect that changes in sea surface temperature (SST) and changes in land-sea thermal contrasts may have played important roles in generating such hydroclimatic differences between ISM and EASM areas.

Conclusions

We studied ISM precipitation over the past ~3500 yr recorded in sediments from Lake Erhai, southwestern China. Our results suggest a long-term decrease in ISM intensity over the late Holocene as inferred from pollen records and physical and chemical proxy indices. For example, the pollen concentrations of conifer trees, broadleaf trees, and herbs clearly declined over the late Holocene; while other proxy indices, including sediment grain size, TOC, and elemental concentrations (e.g., Fe, Al) also indicate decreasing ISM intensity during the same period. One striking feature is that the medieval climate at Lake Erhai was much drier than those of the earlier and later periods. Such a dry medieval climatic condition is broadly similar to those over other ISM areas, but differs from those over EASM areas. The LIA at Lake Erhai was characterized as cold and relatively wet, suggesting that ISM precipitation may have increased during this period, which is also different from the cold and dry climatic conditions over EASM areas. We suspect that the changes in SST of the Indo-Pacific oceans and the related land-sea thermal contrasts may be responsible for these climatic differences between the EASM and ISM areas.

Acknowledgments

This work was funded by the Natural Science Foundation of China (Nos.: 41173122; 41473120) and the National Basic Research Program of China (Nos.: 2013CB955903; 2010CB833405).

References

Adhikari, D., Kumon, F., 2001. Climatic changes during the past 1300 years as deduced from the sediments of Lake Nakatsuna, central Japan. Limnology 2, 157–168.
An, Z.S., Clemens, S.C., Shen, J., Qiang, X.K., Jin, Z.D., Sun, Y.B., Prell, W.L., Luo, J.J., Wang, S.M., Xu, H., Cai, Y.J., Zhou, W.J., Liu, X.D., Liu, W.G., Shi, Z.G., Yan, L.B., Xiao, X.Y., Chang, H., Wu, F., Ai, L., Lu, F.Y., 2011. Glacial–interglacial indian summer monsoon dynamics. Science 333, 719–723.
Appleby, P.G., 1978. The calculation of lead-210 dates assuming a constant rate of supply of unsupported ^{210}Pb to the sediment. Catena 5 (1), 1–8.
Bianchi, G.G., McCave, I.N., 1999. Holocene periodicity in North Atlantic climate and deep-ocean flow south of Iceland. Nature 397, 515–517.
Chen, J.A., Wan, G.J., Tang, D.G., 2000. Recent climate changes recorded by sediment grain sizes and isotopes in Erhai Lake. Progress in Natural Science 10, 54–61.
Chen, F., Chen, X., Chen, J., Zhou, A., Wu, D., Tang, L., Zhang, X., Huang, X., Yu, J., 2014. Holocene vegetation history, precipitation changes and Indian Summer Monsoon evolution documented from sediments of Xingyun Lake, south-west China. Journal of Quaternary Science 29 (7), 661–674.
Chetelat, C., Liu, C., Zhao, Z., Wang, Q., Li, S., Li, J., Wang, B., 2008. Geochemistry of the dissolved load of the Changjiang Basin rivers: anthropogenic impacts and chemical weathering. Geochimica et Cosmochimica Acta 72, 4,254–4,277.
Chu, G., Liu, J., Sun, Q., Lu, H., Gu, Z., Wang, W., Liu, T., 2002. The 'mediaeval warm period' drought recorded in Lake Huguangyan, tropical South China. Holocene 12, 511–516.
Dearing, J.A., Jones, R.T., Shen, J., Yang, X., Boyle, J.F., Foster, G.C., Crook, D.S., Elvin, M.J.D., 2008. Using multiple archives to understand past and present climate–human–environment interactions: the lake Erhai catchment, Yunnan Province, China. Journal of Paleolimnology 40, 3–31.
Diaz, H.F., Trigo, R., Hughes, M.K., Mann, M.E., Xoplaki, E., Barriopedro, D., 2011. Spatial and temporal characteristics of climate in medieval times revisited. Bulletin of the American Meteorological Society 92, 1487–1500.
Ge, Q., Fang, X., Zheng, J., 2002. New understandings on the historical temperature changes in China. Progress in Geography 21, 311–317 (In Chinese with English Abstract).
Goldberg, E.D., 1963. Geochronology with ^{210}Pb "radioactive dating". International Atomic Energy Agency Symposium Proceedings, Vienna, pp. 121–131.
Graham, N., Ammann, C., Fleitmann, D., Cobb, K., Luterbacher, J., 2011. Support for global climate reorganization during the "Medieval Climate Anomaly". Climate Dynamics 37, 1217–1245.
Hyodo, M., Yoshihara, A., Kashiwaya, K., Okimura, T., Masuzawa, T., Nomura, R., Tanaka, S., Xing, T.B., Qing, L.S., Jian, L.S., 1999. A Late Holocene geomagnetic secular variation record from Erhai Lake, southwest China. Geophysical Journal International 136, 784–790.
Ji, J., Shen, J., Balsam, W., Chen, J., Liu, L., Liu, X., 2005. Asian monsoon socillations in the northeastern Qinghai–Tibet Plateau since the late glacial as interpreted from visible reflectance of Qinghai Lake sediments. Earth and Planetary Science Letters 233 (1–2), 61–70.
Laird, K.R., Haig, H.A., Ma, S., Kingsbury, M.V., Brown, T.A., Lewis, C.F.M., Oglesby, R.J., Cumming, B.F., 2012. Expanded spatial extent of the Medieval climate anomaly revealed in lake-sediment records across the boreal region in northwest Ontario. Global Change Biology 18 (9), 2,869–2,881.
Li, X., Walker, D., 1986. The plant geography of Yunnan Province, southwest China. Journal of Biogeography 367–397.
Li, X., Shang, X., Zhou, X., Zhang, H., 2006. Integrative method of sieving and heavy liquid in pollen analysis of loess-data analysis and processing. Arid Land Geography 29, 663–667 (In Chinese with English Abstract).
Li, S.L., Calmels, D., Han, G., Gaillardet, J., Liu, C.Q., 2008. Sulfuric acid as an agent of carbonate weathering constrained by $\delta^{13}C_{DIC}$: examples from Southwest China. Earth and Planetary Science Letters 270 (3–4), 189–199.

https://doi.org/10.1016/j.yqres.2014.12.004 Published online by Cambridge University Press

Liu, Y., An, Z., Linderholm, H.W., Chen, D., Song, H., Cai, Q., Sun, J., Tian, H., 2009. Annual temperatures during the last 2485 years in the mid-eastern Tibetan Plateau inferred from tree rings. Science in China (Series D) 52, 348–359.
Liu, B., Xu, H., Lan, J., Sheng, E., Che, S., Zhou, X., 2014a. Biogenic silica content of Lake Qinghai sediments and its environmental significance. Frontiers of Earth Science http://dx.doi.org/10.1007/s11707-014-0440-0.
Liu, J., Chen, F., Chen, J., Zhang, X., Liu, J., Bloemendal, J., 2014b. Weakening of the East Asian summer monsoon at 1000–1100 A.D. within the Medieval Climate Anomaly: possible linkage to changes in the Indian Ocean-western Pacific. Journal of Geophysical Research-Atmospheres 119 (5), 2209–2219.
Meyers, P.A., 2003. Applications of organic geochemistry to paleolimnological reconstructions: a summary of examples from the Laurentian Great Lakes. Organic Geochemistry 34, 261–289.
Ming, T., Fang, R., 1982. The vegetation on Cangshan Yunnan and the distribution of Genus Rhododendron. Acta Botanica Yunnanica 4, 383–391 (In Chinese with English Abstract).
Ren, G.Y., 1998. Pollen evidence for increased summer rainfall in the Medieval warm period at Maili, northeast China. Geophysical Research Letters 25, 1931–1934.
Robbins, J.A., Edgington, D.N., 1975. Determination of recent sedimentation rates in Lake Michigan using Pb-210 and Cs-137. Geochimica et Cosmochimica Acta 39, 285–304.
Schrader, J.A., Gardner, S.J., Graves, W.R., 2005. Resistance to water stress of Alnus maritima: intra specific variation and comparisons to other alders. Environmental and Experimental Botany 53 (3), 281–298.
Shen, J., Yang, L., Yang, X., Matsumoto, R., Tong, G., Zhu, Y., Zhang, Z., Wang, S., 2005. Lake sediment records on climate change and human activities since the Holocene in Erhai catchment, Yunnan Province. Science in China (Series D) 48, 353–363.
Shen, J., Jones, R.T., Yang, X.D., Dearing, J.A., Wang, S.M., 2006. The Holocene vegetation history of Lake Erhai, Yunnan province southwestern China: the role of climate and human forcings. Holocene 16, 265–276.
Stine, S., 1994. Extreme and persistent drought in California and Patagonia during Medieval time. Nature 369, 546–549.
Stuiver, M., Reimer, P.J., Bard, E., Beck, J.W., Burr, G.S., Hughen, K.A., Kromer, B., McCormac, G., Van DerPlicht, J., Spurk, M., 1998. Intcal98 radiocarbon calibration, 24,000–0 cal BP. Radiocarbon 40, 1041–1083.
Sun, L., Yan, H., Wang, Y., 2012. South China Sea hydrological changes over the past millennium (in Chinese). Chinese Science Bulletin 57, 1730–1738.
Tan, L., Cai, Y., An, Z., Yi, L., Zhang, H., Qin, S., 2011. Climate patterns in north central China during the last 1800 yr and their possible driving force. Climate of the Past 7, 685–692.
Thompson, L.G., Mosley-Thompson, E., Davis, M.E., Henderson, K.A., Brecher, H.H., Zagorodnov, V.S., Mashiotta, T.A., Lin, P.N., Mikhalenko, V.N., Hardy, D.R., Beer, J., 2002. Kilimanjaro Ice Core Records: Evidence of Holocence Climate Change in Tropical Africa. Science 298, 589–593.
Tong, G., Shi, Y., Wu, R., Yang, X., Qu, W., 1997. Vegetation and climate quantitative reconstruction of Longgan Lake since the past 3000 years. Marine Geology & Quaternary Geology 17, 53–61 (In Chinese with English Abstract).
Verschuren, D., Laird, K.R., Cumming, B.F., 2000. Rainfall and drought in equatorial east Africa during the past 1,100 years. Nature 403, 410–414.
Wang, Y.J., Cheng, H., Edwards, R.L., He, Y.Q., Kong, X.G., An, Z.S., Wu, J.Y., Kelly, M.J., Dykoski, C.A., Li, X.D., 2005. The Holocene Asian monsoon: links to solar changes and North Atlantic climate. Science 308, 854–857.
Wang, R., Dearing, J.A., Langdon, P.G., Zhang, E.L., Yang, X.D., Dakos, V., Scheffer, M., 2012. Flickering gives early warning signals of a critical transition to a eutrophic lake state. Nature 492, 419–422.
Wang, T., Surge, D., Walker, K.J., 2013. Seasonal climate change across the Roman Warm Period/Vandal Minimum transition using isotope sclerochronology in archaeological shells and otoliths, southwest Florida, USA. Quaternary International 308, 230–241.
Wu, J., Lu, R., 2005. Spatial pattern and landscape characteristics in Otindag sandy land during the Medieval Warm Period. Journal of Arid Land Resources and Environment 19, 110–113 (In Chinese with English Abstract).
Xu, Z., Liu, C.Q., 2007. Chemical weathering in the upper reaches of the Xijiang River draining the Yunnan–Guizhou Plateau, Southwest China. Chemical Geology 239 (1–2), 83–95.
Xu, S., Zheng, G.D., 2003. Variations in radiocarbon ages of various organic fractions in core sediments from Erhai Lake, SW China. Geochemical Journal 37, 135–144.
Xu, J., Wan, G., Wang, C., Huang, G., Chen, J., 1999. Vertical distribution of ^{210}Pb and ^{137}Cs and their dating in recent sediments of Lugu Lake and Erhai Lake, Yunnan Province. Journal of Lake Sciences 11, 110–116 (In Chinese with English Abstract).
Xu, H., Ai, L., Tan, L.C., An, Z.S., 2006. Stable isotopes in bulk carbonates and organic matter in recent sediments of Lake Qinghai and their climatic implications. Chemical Geology 235, 262–275.
Xu, H., Liu, B., Wu, F., 2010a. Spatial and temporal variations of Rb/Sr ratios of the bulk surface sediments in Lake Qinghai. Geochemical Transaction 11, 3. http://dx.doi.org/10.1186/1467-4866-11-3.
Xu, H., Liu, X.Y., An, Z.S., Hou, Z.H., Dong, J.B., Liu, B., 2010b. Spatial pattern of modern sedimentation rate of Qinghai Lake and a preliminary estimate of the sediment flux. Chinese Science Bulletin 55, 621–627.
Xu, H., Hong, Y.T., Hong, B., 2012. Decreasing Asian summer monsoon intensity after 1860 AD in the global warming epoch. Climate Dynamics 39, 2079–2088.
Xu, H., Sheng, E.G., Lan, J.H., Liu, B., Yu, K.K., Che, S., 2014. Decadal/multi-decadal temperature discrepancies along the eastern margin of the Tibet plateau. Quaternary Science Reviews 89, 85–93.
Yamada, K., Kamite, M., Saito-Kato, M., Okuno, M., Shinozuka, Y., Yasuda, Y., 2010. Late Holocene monsoonal-climate change inferred from Lakes Ni-no-Megata and San-no-Megata, northeastern Japan. Quaternary International 220, 122–132.
Yang, B., Braeuning, A., Shi, Y., Chen, F., 2004. Evidence for a late Holocene warm and humid climate period and environmental characteristics in the arid zones of northwest China during 2.2–1.8 kyr B.P. Journal of Geophysical Research 109, D02105. http://dx.doi.org/10.1029/2003JD003787.
Yang, B., Wang, J., Brauning, A., Dong, Z., Esper, J., 2009. Late Holocene climatic and environmental changes in arid central Asia. Quaternary International 194, 68–78.
Zeng, Y., Chen, J., Xiao, J., Qi, L., 2013. Non-residual Sr of the sediments in Daihai Lake as a good indicator of chemical weathering. Quaternary Research 79 (2), 284–291.
Zhang, D., 1994. Evidence for the existence of the Medieval Warm Period in China. Climatic Change 26, 289–297.
Zhang, S., Xu, C., Zhong, Z., Ren, T., Jing, Y., 1993. Determination of sedimentation rate and dating of sediment in Erhai Lake with ^{210}Pb and ^{137}Cs dating methods. Radiation Protection 13, 453–457 (In Chinese with English Abstract).
Zhang, Z., Wu, R., Shen, J., Wu, Y., Zhu, Y., Pan, H., 2000. Lacustrine records of climatic change and human activities in the catchment of Erhai Lake, Yunnan Province since the past 1800 years. Journal of Lake Sciences 12, 297–303 (In Chinese with English Abstract).
Zhang, Q.B., Cheng, G.D., Yao, T.D., Kang, X.C., Huang, J.G., 2003. A 2,326-year tree-ring record of climate variability on the northeastern Qinghai–Tibetan Plateau. Geophysical Research Letters 30. http://dx.doi.org/10.1029/2003gl017425.
Zhang, R., Li, S., Jiang, Y., 2007. Introduction of *eucalyptus* in Yunnan and analysis on development status. Journal of West China Forestry Science 36, 97–102 (In Chinese with English Abstract).
Zhang, Y., Kong, Z.C., Yan, S., Yang, Z.J., Ni, J., 2009. "Medieval warm period" on the northern slope of central Tianshan mountains, Xinjiang, NW China. Geophysical Research Letters 36, L11702. http://dx.doi.org/10.1029/2009GL037375.
Zhao, H., Wang, S., Zhao, M., Jiao, L., Liu, B., Jin, X., 2011. Relationship between the DO and the environmental factors of the water body in Lake Erhai. Environmental Sciences 32 (7), 1952–1959 (In Chinese with English Abstract).
Zhou, X., Li, X., 2012. Variations in spruce (Picea sp.) distribution in the Chinese Loess Plateau and surrounding areas during the Holocene. Holocene 22 (6), 687–696.
Zhou, Y.L., Lu, H.Y., Mason, J., Miao, X.D., Swinehart, J., Goble, R., 2008. Optically stimulated luminescence dating of aeolian sand in the Otindag dune field and Holocene climate change. Science in China (Series D) 51, 837–847.
Zhou, X.J., Zhao, P., Liu, G., Zhou, T.J., 2011. Characteristics of decadal–centennial-scale changes in East Asian summer monsoon circulation and precipitation during the Medieval Warm Period and Little Ice Age and in the present day. Chinese Science Bulletin 56 (28–29), 3003–3011.

https://doi.org/10.1016/j.yqres.2014.12.004 Published online by Cambridge University Press